Geoid
Journal of Geodesy and Geomatics

Geoid Vol. 20, No. 2, 2025, 1-8

P-ISSN: 1858-2281; E-ISSN: 2442-3998

A Look at the Time Series of NDVI and NDWI at a Wildfire Site in California, USA

Indumathi Jeyachandran*[1]
[1] Department of Civil and Environmental Engineering, San Jose State University, One Washington Square, San Jose, CA -95192
*Corresponding author: Indumathi.jeyachandran@sjsu.edu

Received: 29072024; Revised: 21072025; Accepted: 21072025; Published: 05092025

Abstract: Wildfires are a recurring and increasingly severe hazard in California, with substantial ecological, economic, and social consequences. The Thomas Fire of December 2017, the eighth largest in state history, caused extensive vegetation loss and infrastructure damage, emphasizing the need for effective monitoring of fire-prone landscapes. Vegetation health and canopy water content are key determinants of wildfire susceptibility. Stressed or desiccated vegetation is more flammable, while healthy, well-hydrated vegetation is less likely to ignite. Using remote sensing, these conditions can be monitored across large areas and over time. This study analyzes Landsat 8 OLI and TIRS time-series data (2013–2017) for the Thomas Fire site. Data were processed in Esri ArcMap 10.7 to derive the Normalized Difference Vegetation Index (NDVI), indicating vegetation vigor, and the Normalized Difference Water Index (NDWI), indicating canopy moisture. Results show that declines in NDVI and NDWI preceded the fire, suggesting that Landsat-derived indices can support wildfire risk assessment by identifying vegetation stress and low canopy water content as early warning indicators.

Keywords : NDVI; NDWI; wildfire; canopy water content; vegetation health; Thomas Fire

Jeyachandran, I. (2025). A Look at the Time Series of NDVI and NDWI at a Wildfire Site in California, USA. *Geoid, 20* (2), 1-8.

Introduction

California has experienced some of the deadliest wildfires in recent years. Some of the deadliest wildfires in California include Camp fire and Thomas Fire. Wildfire season in California starts in late Spring around May and runs through December. In 2023, the number of wildfire incidents was 7386 and around 332,822 Acres were burned, and this was significantly less than the fiver year average (CAL FIRE, 2025). The fire season in 2023 was significantly less destructive than the other years owing to weather conditions and proactive management. In 2024, the number of wildfire incidents was 8,024 and 1 million acres were burned (CAL Fire, 2025). Wildfire activity in 2024 was significantly higher than the previous years and this has been attributed to hotter than usual temperatures in June and an increase in fine fuels. The largest wildfire in 2024 was the Park Fire in Southern California (Butte County) which started in July 2024 and destroyed 429, 603 acres. 2025 has seen some unprecedented early fires starting in January and till date there has been 2990 wildfire incidents (CAL FIRE, 2025). Wild-fire has profound impacts on soil properties and stability (Francos et al., 2016), soil microbial communities (Prendergast-Miller et al., 2017), hydrological processes (Mahat et al., 2015; Pimentel et al., 2014; Nunes et al., 2020), infant health (McCoy et al., 2021), health of fire fighters (Navarro, 2020).

State of California, Department of Forestry and Fire Protection (CAL FIRE) has been enacting various preventive measures to manage wildfire. These preventive measures include fuels reduction which involves reducing overgrown vegetation, use of prescribed fires, requiring campfire permits for campfires in public lands. Drier vegetation subjected to hotter air temperatures contribute to an increase in wildfires. Monitoring vegetation health and water stress, through the use of remote sensing data-derived indices will be instrumental in identifying areas vulnerable to wildfire occurrence, and in mitigating impacts of wildfire. Remote Sensing da-ta-derived indices NDVI and NDWI have been used for a wide array of applications as listed in the following paragraphs.

Normalized Difference Vegetation Index is an indicator of vegetation greenness and vegetation health (Tucker, 1979). The value of NDVI ranges from -1 to +1. Higher values of NDVI indicates greener vegetation. NDWI is an indicator of the vegetation water content and is less impacted by atmospheric scattering effects (Gao, 1996). The value of NDWI ranges from -1 to +1. Lower values of NDWI indicate water-stressed vegetation. The correlation between Landsat derived NDVI, NDWI and vegetation water content has been explored and NDWI was found to be more sensitive to changes in vegetation water content (Jackson et al., 2004). NDWI has been found to be effective in the detection and monitoring of vegetation soil moisture (Jackson et al., 2004; Chen et al., 2005).

NDVI derived from remote sensing data has been extensively used for vegetation drought monitoring (Kogan, 1995; Ji & Peters, 2003; Gu et al., 2007; Gu et al., 2008; Zhang et al., 2013). NDVI has also been found to correlate with crop productivity (Naser et al., 2020) and has been used for studying vegetation degradation (Zhumanova et al., 2018). NDVI and NDWI derived from MODIS data have been used for monitoring live fuel moisture in Southern California and NDWI was found to correlate significantly with live fuel moisture (Dennison et al., 2005). In a study in a walnut orchard in Central California, NDVI from high-resolution multispectral imagery was used to assess the correlation between NDVI, red edge indices and stem water potential, the results indicate a correlation with a R Square value of 0.63 (Wang & Jin, 2023). In a study involving sampling sites in the western US, the correlation between Landsat-5 surface reflectance-derived NDVI, NDWI, other spectral indices and field sampled Live Fuel Moisture Content (LFMC) was explored (Garcia et al., 2020). The LFMC product estimated from the spectral indices using linear regression model, were used in fire behavior modeling (Garcia et al., 2020).

In this paper the relationship between vegetation health, vegetation water stress and wildfire occurrences is explored through the use of Landsat 8 surface reflectance-derived NDVI and NDWI. The question primarily answered through this re-search is "Can NDVI and NDWI be used to identify areas vulnerable to wildfire triggers and occurrences?" To answer this question time series of NDVI and NDWI images were created and analyzed to assess vegetation health and water stress prior to the occurrence of the deadly Thomas Fire, which started on December 4, 2017. Further, the indices were analyzed in conjunction with meteorological data to identify triggers of wildfire attributed to high windspeeds, and extended periods of high temperatures.

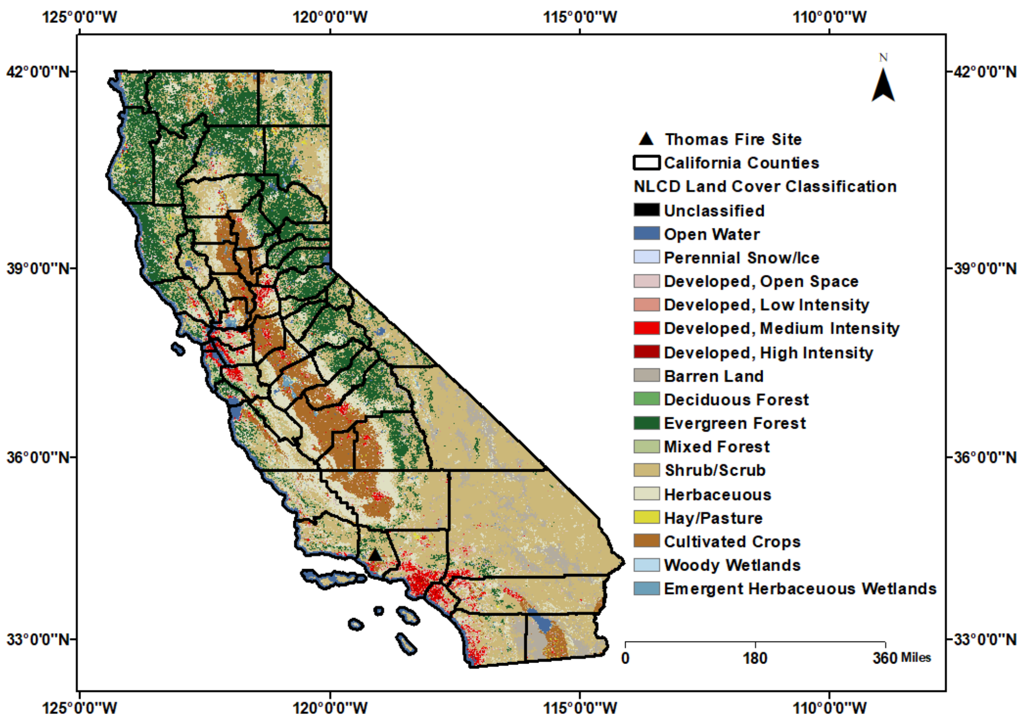

Figure 1. Land Cover Map of the Thomas Fire Site.

Study Area, Data and Method

Study Area

Ventura county prone to the deadliest Thomas Fire, and Woolsey fire was used for this research. Specifically, the Thomas Fire site was used as the case study site. Latitude and longitude of the study site are 34.41521 °N and 119.099124 °W. Land cover map of the Thomas Fire site is shown in Figure 1. The land cover data was downloaded from the from the Multi- Resolution Land Characteristics Consortium Website. Land cover class at the Thomas Fire site is predominantly shrub/scrub.

Data Used

Landsat 8 OLI and TIRS Level -1 GeoTIFF data was downloaded from USGS GloVis Viewer. A filter was set in GloVis to identify and download Landsat scenes with cloud coverless than 20 percent. 75 Landsat scenes acquired in the months of April (04/01) through November (11/30) for the years 2013 to 2017, were downloaded and processed. Additionally, Landsat 8 OLI and TIRS scene was downloaded and processed for December 2, 2017, 2 days prior to the occurrence of the Thomas Fire. Information on Landsat data used for this study is in Table 1.

Table 1. Landsat-8 OLI and TIRS Study Site Specific Information

Year	Latitude (N) and Longitude (W) of the Study Site	Landsat 8 Path and Row	Landsat Sensors	Landsat Scene acquisition time period	Number of Landsat Scenes Processed
2013	34.41521 (N) and 119.099124 (W)	Path = 41, Row = 36	OLI and TIRS	04/01/2013 to 11/30/2013	11
2014	34.41521 (N) and 119.099124 (W)	Path = 41, Row = 36	OLI and TIRS	04/01/2014 to 11/30/2014	9
2015	34.41521 (N) and 119.099124 (W)	Path = 41, Row = 36	OLI and TIRS	04/01/2015 to 11/30/2015	11
2016	34.41521 (N) and 119.099124 (W)	Path = 41, Row = 36	OLI and TIRS	04/01/2016 to 11/30/2016	9
2017	34.41521 (N) and 119.099124 (W)	Path = 41, Row = 36	OLI and TIRS	04/01/2017 to 12/02/2017	13

Methodology

The Landsat data scenes downloaded from USGS GloVis Server (https://glovis.usgs.gov/). During the process of downloading the data, a filter was set to exclude any Landsat scene with cloud cover greater than 20%. Total of 75 Landsat 8 scenes were downloaded. Further, the Landsat scenes was processed in ArcMap 10.7. Landsat 8 surface reflectance data was used for computing NDVI and NDWI.

NDVI, NDWI, images were generated using Spatial Analyst raster calculator tool in ArcGIS. The process to generate NDVI and NDWI images was automated using Model Builder tools in ArcMap 10.7 to process multiple scenes A toolbox for water stress analysis was created. A toolbox for water stress analysis was created in ArcMap 10.7. The toolbox consists of NDVI tool, and NDWI tool created using Model Builder. The WaterStress Analysis toolbox, and the NDVI and NDWI model builder tools are shown in Figures 2, 3, and 4.

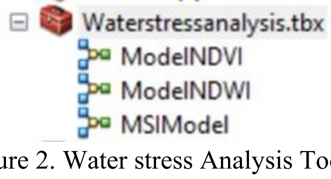

Figure 2. Water stress Analysis Toolbox

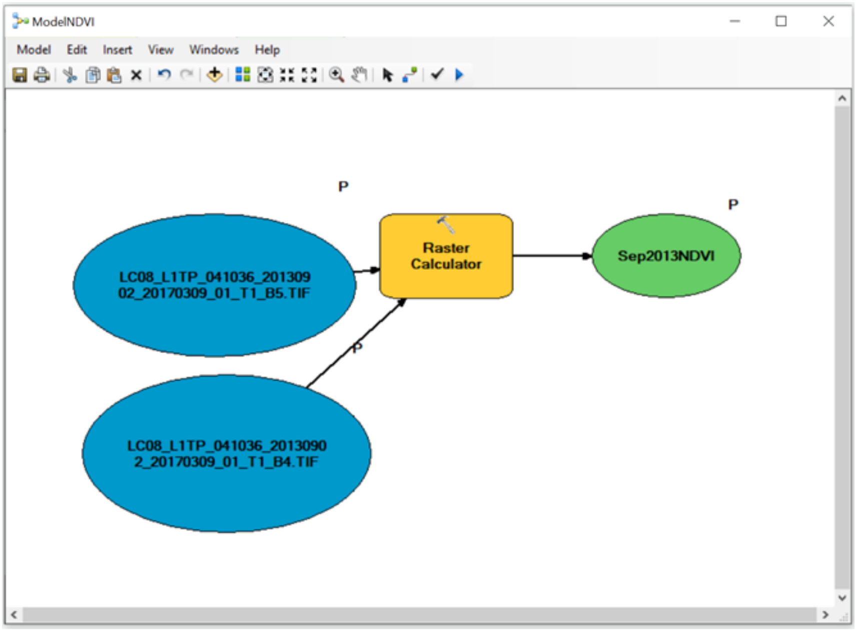

Figure 3. Model Builder Tool to Compute NDVI

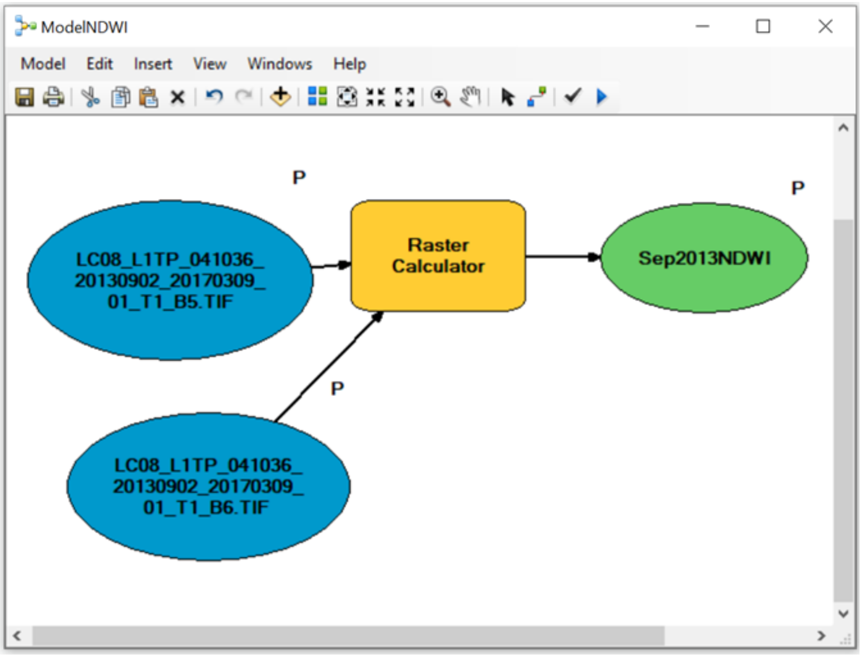

Figure 4. Model Builder Tool to Compute NDWI

NDVI is computed using the reflectance in the red and near-infrared bands. In Landsat 8, bands 4 and 5 correspond to red and near-infrared (NIR) bands, respectively. In this paper, NDVI is estimated using band 4 (0.636 to 0.673 µm) and band 5 (0.851 to 0.879 µm) of Landsat-8 OLI and TIRS data.

$$NDVI = (\rho_{NIR} - \rho_{RED})/ (\rho_{NIR} + \rho_{RED}) \qquad (1)$$

The raster calculator equation used to compute NDVI was:

$$NDVI = (Band\ 5 - Band\ 4)/(Band\ 5 + Band\ 4) \qquad (2)$$

NDWI was proposed to measure water content in vegetation (Gao 1996). NDWI is computed using the reflectance in the near-infrared (NIR) and short-wave infrared (SWIR) bands. In this paper, NDWI is estimated using band 5 (0.851 to 0.879 µm) and band 6 (1.566 to 1.651 µm) of Landsat 8 OLI and TIRS data.

$$NDWI = (\rho_{NIR} - \rho_{SWIR})/ (\rho_{NIR} + \rho_{SWIR}) \qquad (3)$$

The raster calculator equation used to compute NDWI was:

$$NDWI = (Band\ 5 - Band\ 6)/ (Band\ 5 + Band\ 6) \tag{4}$$

NDVI and NDWI images were generated to the extent of each Landsat scene. In order to analyze NDVI and NDWI at the Thomas Fire site, the NDVI and NDWI values of 6 pixels in and around the vicinity of the site was averaged to find a single representative value of NDVI and NDWI. Pixel based values of NDVI and NDWI used to compute the averaged NDVI and NDWI values at the Thomas Fire site is shown in Figures 5 and 6.

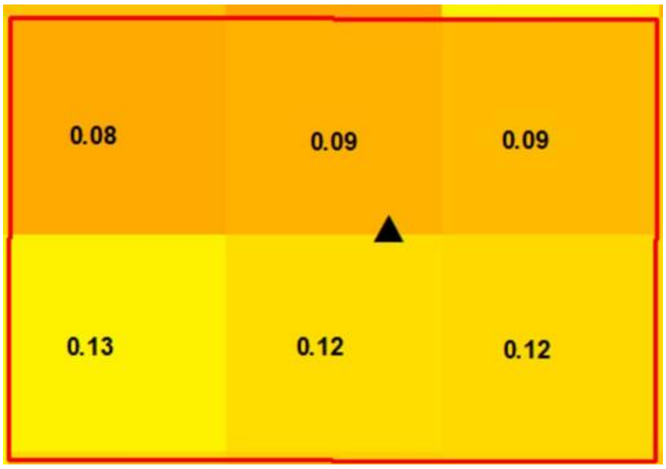

Figure 5 . Pixel based NDVI Values in and around the Thomas Fire site

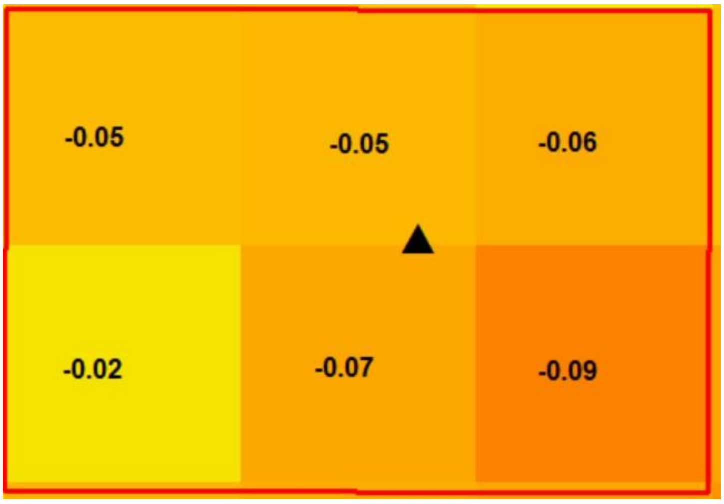

Figure 6. Pixel based NDWI Values in and around the Thomas Fire site

Results and Discussion

NDVI values at the Thomas Fire site was observed to decrease gradually from April through November. This trend was observed across all the years. The decreasing trend of NDVI values from April through November during the time period of 2013 through 2017, is shown in Figure 7a. The NDVI values at the Thomas Fire site on December 2, 2017 was 0.1. The NDWI value at the Thomas Fire Site has a trend similar to that of NDVI and is shown in Figure 7b. The NDWI value on December 2, 2017 was estimated to be -0.0555 and this value indicates water stressed vegetation. The values of NDVI and NDWI on December 2, 2017, two days prior to the Thomas Fire incident indicates dry and water stressed vegetation. The mean value of NDVI and NDWI at the Thomas Fire site from April through December 2, 2017 is shown in Table 2.

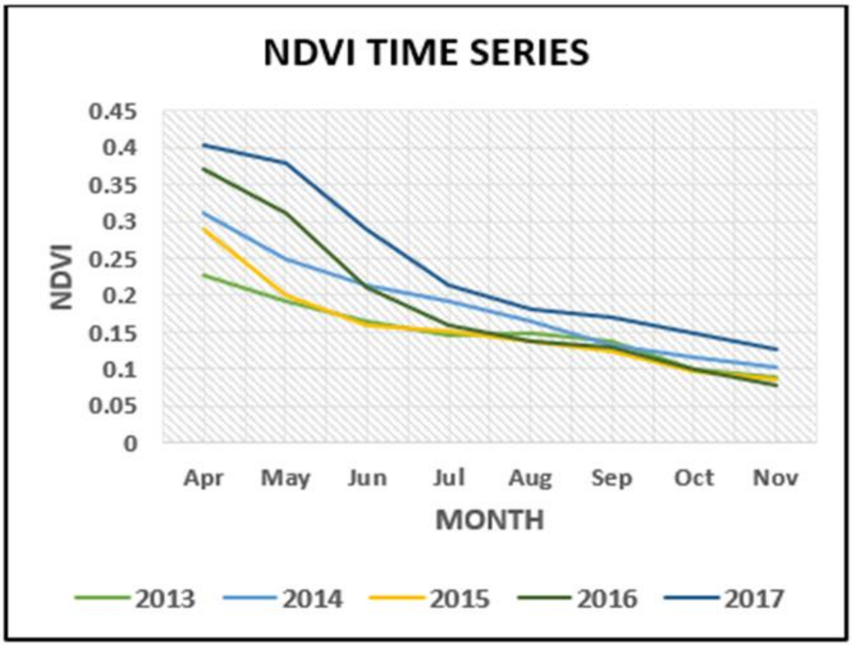

(a)

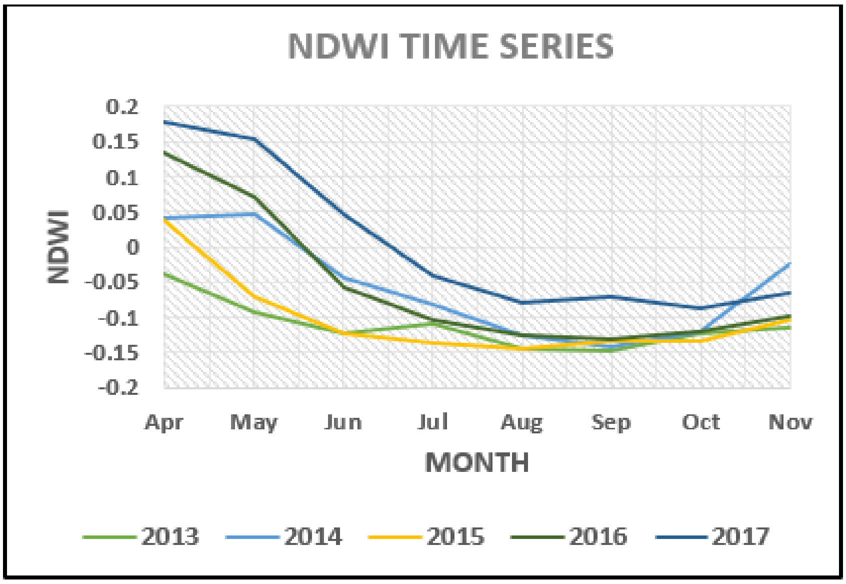

(b)

Figure 7. Trend of NDVI and NDWI Values from April through November, 2017. (a) NDVI Values. (b) NDWI Values.

Table 2. NDVI and NDWI values at the Thomas Fire Site in 2017

Date	Mean NDVI	Mean NDWI
4/22/2017	0.4027	0.1778
5/19/2017	0.3780	0.1542
6/9/2017	0.3083	0.0772
6/25/2017	0.2713	0.0158
7/11/2017	0.2167	-0.0308
7/27/2017	0.2083	-0.0535
8/12/2017	0.1897	-0.0688
8/28/2017	0.1705	-0.0888
9/13/2017	0.1688	-0.0697
10/6/2017	0.1670	-0.0923
10/22/2017	0.1300	-0.0828
11/16/2017	0.1260	-0.0660
12/2/2017	0.100	-0.0555

The daily temperature, precipitation, and wind speed data for the Thomas Fire site's nearest weather station (Oxnard Ventura Co Airport, station ID: USW00093110) were obtained from NOAA National Centers for Environmental Information. The analysis of temperature data from April through December of 2017 for the Thomas Fire site indicates a total 143 days out of 365 days with temperature greater than 85° Fahrenheit . Also, there was no significant rain from April through December of 2017. Los Angeles and Ventura counties are prone to strong Santa Ana winds. The fastest five-minute wind speed on the day of the Thomas Fire incident was 42.9 miles/hour.

Based on the results from the study, it can be inferred that the Thomas fire site exhibited significantly low values of NDVI and NDWI which corresponds to dry and water stressed vegetation and when the site was subjected to high winds the wildfire was triggered. This study indicates the potential of Landsat 8 surface reflectance–derived indices of NDVI and NDWI in identifying areas with dry and water stressed vegetation which are more susceptible to triggers of wildfire.

Conclusions

The results of the study demonstrate the potential to use Landsat 8 surface reflectance-derived NDVI and NDWI for identifying areas susceptible to wildfires. Identifying and monitoring areas vulnerable to wildfires using NDVI and NDWI will be of vital use to local and state government agencies to mitigate wildfire risk hazards. Future study would extend the analysis to other case study sites in California and explore correlations between NDVI, NDWI and wildfire intensity.

Acknowledgment

This research was funded by SJSU Charles W. Davidson College of Engineering.

References

CAL FIRE. (2025). The California Department of Forestry and Fire Protection. https://www.calfire.ca.gov/safety/firesafetytips.

Chen, D., Huang, J., & Jackson, T. J. (2005). Vegetation water content estimation for corn and soybeans using spectral indices derived from MODIS near- and short-wave infrared bands. *Remote Sensing of Environment*, *98*(2), 225-236. https://doi.org/https://doi.org/10.1016/j.rse.2005.07.008

Dennison, P. E., Roberts, D. A., Peterson, S. H., & Rechel, J. (2005). Use of Normalized Difference Water Index for monitoring live fuel moisture. *International Journal of Remote Sensing*, *26*(5), 1035-1042. https://doi.org/10.1080/0143116042000273998

Francos, M., Pereira, P., Alcañiz, M., Mataix-Solera, J., & Úbeda, X. (2016). Impact of an intense rainfall event on soil properties following a wildfire in a Mediterranean environment (North-East Spain). *Science of The Total Environment*, *572*, 1353-1362. https://doi.org/https://doi.org/10.1016/j.scitotenv.2016.01.145

Gao, B.-c. (1996). NDWI—A normalized difference water index for remote sensing of vegetation liquid water from space. *Remote Sensing of Environment*, *58*(3), 257-266. https://doi.org/https://doi.org/10.1016/S0034-4257(96)00067-3

García, M., Riaño, D., Yebra, M., Salas, J., Cardil, A., Monedero, S., Ramirez, J., Martín, M. P., Vilar, L., Gajardo, J., & Ustin, S. (2020). A Live Fuel Moisture Content Product from Landsat TM Satellite Time Series for Implementation in Fire Behavior Models. *Remote Sensing*, *12*(11), 1714. https://www.mdpi.com/2072-4292/12/11/1714

Gu, Y., Brown, J. F., Verdin, J. P., & Wardlow, B. (2007). A five-year analysis of MODIS NDVI and NDWI for grassland drought assessment over the central Great Plains of the United States. *Geophysical Research Letters*, *34*(6). https://doi.org/https://doi.org/10.1029/2006GL029127

Gu, Y., Hunt, E., Wardlow, B., Basara, J. B., Brown, J. F., & Verdin, J. P. (2008). Evaluation of MODIS NDVI and NDWI for vegetation drought monitoring using Oklahoma Mesonet soil moisture data. *Geophysical Research Letters*, *35*(22). https://doi.org/https://doi.org/10.1029/2008GL035772

Jackson, T. J., Chen, D., Cosh, M., Li, F., Anderson, M., Walthall, C., Doriaswamy, P., & Hunt, E. R. (2004). Vegetation water content mapping using Landsat data derived normalized difference water index for corn and soybeans. *Remote Sensing of Environment*, *92*(4), 475-482. https://doi.org/https://doi.org/10.1016/j.rse.2003.10.021

Ji, L., & Peters, A. J. (2003). Assessing vegetation response to drought in the northern Great Plains using vegetation and drought indices. *Remote Sensing of Environment*, *87*(1), 85-98. https://doi.org/https://doi.org/10.1016/S0034-4257(03)00174-3

Kogan, F. N. (1995). Droughts of the Late 1980s in the United States as Derived from NOAA Polar-Orbiting Satellite Data. *Bulletin of the American Meteorological Society*, *76*(5), 655-668. https://doi.org/10.1175/1520-0477(1995)076<0655:Dotlit>2.0.Co;2

Mahat, V., Anderson, A., & Silins, U. (2015). Modelling of wildfire impacts on catchment hydrology applied to two case studies. *Hydrological Processes*, *29*(17), 3687-3698.

McCoy, S. J., & Zhao, X. (2021). Wildfire and infant health: a geospatial approach to estimating the health impacts of wildfire smoke exposure. *Applied Economics Letters*, *28*(1), 32-37. https://doi.org/10.1080/13504851.2020.1730747

Naser, M. A., Khosla, R., Longchamps, L., & Dahal, S. (2020). Using NDVI to Differentiate Wheat Genotypes Productivity Under Dryland and Irrigated Conditions. *Remote Sensing*, *12*(5), 824. https://www.mdpi.com/2072-4292/12/5/824

Navarro, K. (2020). Working in Smoke:: Wildfire Impacts on the Health of Firefighters and Outdoor Workers and Mitigation Strategies. *Clinics in chest medicine*, *41*(4), 763-769.Nunes, J. P., Bernard-Jannin, L., Rodríguez-Blanco, M. L., Boulet, A. K., Santos, J. M., & Keizer, J. J. (2020). Impacts of wildfire and post-fire land management on hydrological and sediment processes in a humid Mediterranean headwater catchment. *Hydrological Processes*, *34*(26), 5210-5228.

Pimentel, R., & Arheimer, B. (2021). Hydrological impacts of a wildfire in a Boreal region: The Västmanland fire 2014 (Sweden). *Science of The Total Environment*, *756*, 143519. https://doi.org/https://doi.org/10.1016/j.scitotenv.2020.143519

Prendergast-Miller, M. T., de Menezes, A. B., Macdonald, L. M., Toscas, P., Bissett, A., Baker, G., Farrell, M., Richardson, A. E., Wark, T., & Thrall, P. H. (2017). Wildfire impact: Natural experiment reveals differential short-term changes in soil microbial communities. *Soil Biology and Biochemistry*, *109*, 1-13. https://doi.org/https://doi.org/10.1016/j.soilbio.2017.01.027

Tucker, C. J. (1979). Red and photographic infrared linear combinations for monitoring vegetation. *Remote Sensing of Environment*, *8*(2), 127-150. https://doi.org/https://doi.org/10.1016/0034-4257(79)90013-0

Wang, K., & Jin, Y. (2023). Mapping Walnut Water Stress with High Resolution Multispectral UAV Imagery and Machine Learning. arXiv preprint. https://doi.org/10.48550/arXiv.2401.01375

Yang, L., Wylie, B. K., Tieszen, L. L., & Reed, B. C. (1998). An Analysis of Relationships among Climate Forcing and Time-Integrated NDVI of Grasslands over the U.S. Northern and Central Great Plains. *Remote Sensing of Environment*, *65*(1), 25-37. https://doi.org/https://doi.org/10.1016/S0034-4257(98)00012-1

Zhang, F., Zhang, L.-w., Wang, X.-z., & Hung, J.-f. (2013). Detecting Agro-Droughts in Southwest of China Using MODIS Satellite Data. *Journal of Integrative Agriculture*, *12*(1), 159-168. https://doi.org/https://doi.org/10.1016/S2095-3119(13)60216-6

Zhumanova, M., Mönnig, C., Hergarten, C., Darr, D., & Wrage-Mönnig, N. (2018). Assessment of vegetation degradation in mountainous pastures of the Western Tien-Shan, Kyrgyzstan, using eMODIS NDVI. *Ecological Indicators*, *95*, 527-543. https://doi.org/https://doi.org/10.1016/j.ecolind.2018.07.060